Bioorganic & Medicinal Chemistry 19 (2011) 429–439

Contents lists available at ScienceDirect

Bioorganic & Medicinal Chemistry

journal homepage: www.elsevier.com/locate/bmc

Synthesis and biological evaluation of 7-substituted-1-(3-bromophenylamino)isoquinoline-4-carbonitriles as inhibitors of myosin light chain kinase and epidermal growth factor receptor

Haridas B. Rode [a], Martin L. Sos [b], Christian Grütter [a], Stefanie Heynck [b], Jeffrey R. Simard [a], Daniel Rauh [a,*]

[a] Chemical Genomics Centre of the Max Planck Society, Otto-Hahn-Strasse 15, 44227 Dortmund, Germany
[b] Max Planck Institute for Neurological Research with Klaus-Joachim-Zülch Laboratories of the Max Planck Society and the Medical Faculty of the University of Köln, Gleueler Strasse 50, 50931 Köln, Germany

ARTICLE INFO

Article history:
Received 2 September 2010
Revised 2 November 2010
Accepted 4 November 2010
Available online 10 November 2010

Keywords:
Kinase inhibitors
Inhibitor profiling
Medicinal chemistry

ABSTRACT

Here we present the synthesis and biological activity of a series of 7-substituted-1-(3-bromophenylamino)isoquinoline-4-carbonitriles as inhibitors of myosin light chain kinase (MLCK) and the epidermal growth factor receptor kinase (EGFR). The inhibitory effect of these molecules was found to be dependent on the nature of the substituents at the 7-position of the isoquinoline scaffold.

1. Introduction

Protein kinases are crucial enzymes for the regulation of nearly every cellular signaling event, including proliferation and apoptosis. Kinase function has been found to be disregulated in many diseases such as cancer, inflammation, diabetes and central nervous system disorders.[1] The detailed understanding of kinase malfunction in the onset and progression of cancer led to the development of potent kinase inhibitors as a means of novel targeted therapies currently in clinical use.[2] Furthermore, kinase inhibitors serve as powerful tool compounds in chemical biology research to probe and dissect enzymatic kinase function in complex cellular systems.[3] An increasing number of biological studies investigating the role of the Ca^{2+}/calmodulin dependent kinase smMLCK (smooth muscle myosin light chain kinase, also referred to as MLCK) in metastatic cancer cell invasion, regulation of epithelial cell survival, hypertension and inflammatory bowel diseases reflect its emergence as a potentially novel therapeutic target.[4–8] MLCK is a serine/threonine kinase and transfers the γ-phosphate from ATP to a serine residue of the 20-kD regulatory light chain of myosin (MLC_{20}).[4,5] Phosphorylated myosin interacts with actin filaments, resulting in the contraction of smooth muscle fibers.[9] Thus, the phosphorylation of myosin is a major regulatory pathway in smooth muscle contraction and is complemented by Ca^{2+}-independent Rho kinases (ROCK I and ROCK II), which phosphorylate and inactivate myosin light chain phosphatase to prevent uncontrolled muscle fiber relaxation.[10,11] Interestingly, MLCK-dependent increases in myosin ATPase activity have also been observed in the contraction and migration of non-muscle cells, highlighting an important role for MLCK in muscle as well as non-muscle cells.[12–14]

Despite these many biological roles, only a handful of small organic molecules have been reported so far to be active as MLCK inhibitors and might qualify as probe molecules to study the diverse functional roles of this key kinase in more detail (Fig. 1).[15–19] The naphthalene sulfonamides W-7, ML-7, and ML-9, which are close analogs of the marketed vasodilator and ROCK II kinase inhibitor Fasudil (HA-1077), as well as the microbial metabolites K-252a[18] and Wortmannin[19] have been shown to be ATP-competitive inhibitors of MLCK.[15] Additionally, studies on the auto-inhibition mechanism of MLCK led to the identification of potent, peptide-based inhibitors.[17] Here we report the identification and further development of 7-substituted-1-(3-bromophenylamino)isoquinoline-4-carbonitriles as a novel class of selective MLCK inhibitors. Interestingly, one of these compounds was also found to be an inhibitor of a clinically relevant target in cancer, namely the epidermal growth factor receptor (EGFR), both in biochemical and cellular assays.

* Corresponding author. Tel.: +49 (0)231 9742 6480; fax: +49 (0)231 9742 6479.
E-mail address: daniel.rauh@cgc.mpg.de (D. Rauh).

0968-0896/$ - see front matter © 2010 Elsevier Ltd. All rights reserved.
doi:10.1016/j.bmc.2010.11.007

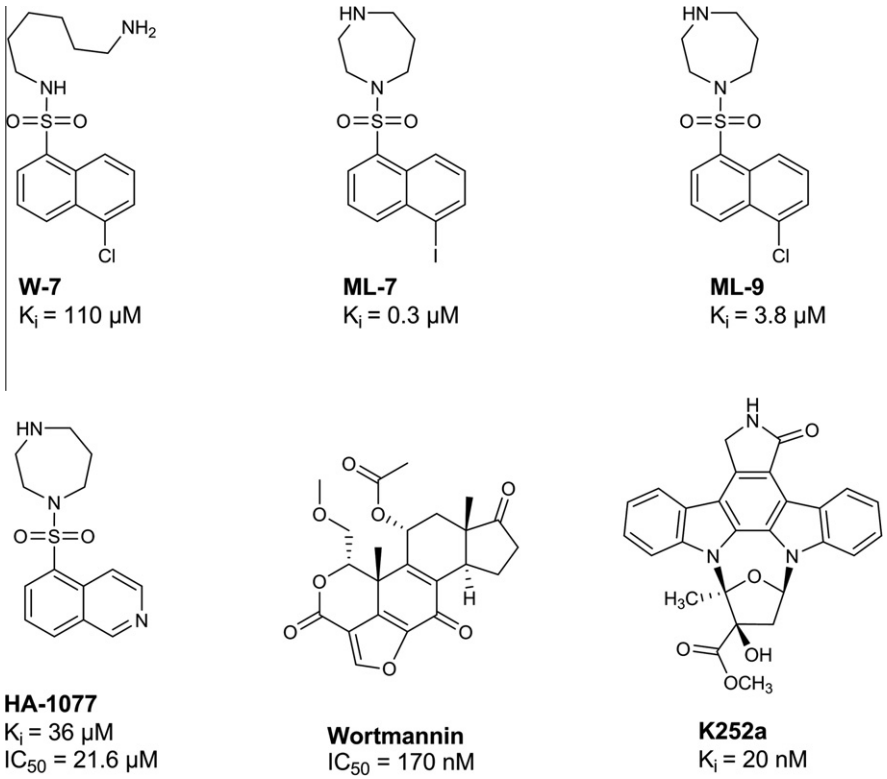

Figure 1. Structures of known ATP-competitive MLCK inhibitors. W-7, ML-7 and ML-9 are close analogs of the Rho kinase (ROCK II) inhibitor Fasudil (HA-1077). Wortmanin and K-252a are metabolites obtained from microorganisms and are potent but unselective inhibitors of MLCK.[15–19]

2. Results and discussion

2.1. Screening for inhibitors of MLCK

In order to identify novel inhibitors of MLCK, we screened a focused compound library in a 384-well format by detecting substrate phosphorylation in the presence of Ca^{2+}/calmodulin and using homogeneous time-resolved fluorescence (HTRF) as a readout. We identified 7-substituted-1-(3-bromophenylamino)isoquinoline-4-carbonitriles **8** and **9** as weak primary hits. Although these two molecules differ in the extent of saturation of the side chain attached at the 7-position of the isoquinoline core, they were equipotent with IC_{50} values of 25 and 24 μM, respectively (Table 1). To the best of our knowledge, 7-amino substituted isoquinoline-4-carbonitriles were not previously reported as MLCK inhibitors in literature so we set out to further develop these hits into more potent inhibitors.

2.2. Profiling for kinase inhibitor selectivity

In order to gain more insights into their selectivity profiles and SAR, we profiled the identified hit molecules **8** and **9** against a panel of 95 kinases at a concentration of 10 μM (National Centre for Protein Kinase Profiling, University of Dundee, UK) (Fig. 2). Despite the different substituents at the 7-position of the isoquinoline ring, the compounds show similar selectivity profiles with preferred inhibition of MLCK. While **8** also strongly inhibits the Ca^{2+}/calmodulin dependent kinases PHK and CAMK1, **9** shows preferential inhibition of the receptor tyrosine kinase HER4. Interestingly, both molecules fail to inhibit the Ca^{2+}/calmodulin dependent protein kinase kinase β (CAMKKβ). With the exception of HER4, all kinases inhibited by **8** or **9** posses a large hydrophobic amino acid at the gatekeeper position. The gatekeeper is located at the back of the ATP binding pocket and adjacent to the hinge region. The size and polarity of this amino acid is well-known for influencing inhibitor affinity and selectivity profiles amongst kinases.[2]

2.3. Synthesis and SAR of a focused library of 7-substituted-3-bromophenylamino-isoquinoline-4-carbonitriles

Based on this initial SAR and to further optimize compound potency, we synthesized a focused library of 3-bromophenylamino-isoquinoline-4-carbonitriles with various substituents at the 7-position of the isoquinoline core (Scheme 1). The synthesis commenced with the nitration of commercially available isoquinoline-1-one **1** to produce the 5- and 7-nitro positional isomers **2** and **3**, which were separated by repeated column chromatography. The 7-nitro isomer **3** was brominated to give **4**. Palladium-catalyzed cyanation of **4** with $Zn(CN)_2$ as the cyanide source and S-Phos as the ligand produced **5** in moderate yield. Alternatively, the cyanation reaction could be performed with the assistance of microwaves, but resulted in significantly lower yields. Chlorination of **5** with phosphorous oxychloride followed by treatment with *m*-bromoaniline resulted in analog **6**. Selective reduction of the nitro group in the presence of bromine was then successfully fulfilled by treating **6** with $SnCl_2$. The resulting amine **7** was coupled with different acids or treated with the corresponding acid chlorides to generate a focused library of 7-substituted-1-(3-bromophenylamino)isoquinoline-4-carbonitriles. All compounds were tested for inhibition of MLCK (Table 1). The introduction of a *N*-methylpiperazine in the 7-position of the isoquinoline core (**11**) significantly enhanced potency (threefold) against MLCK when compared to primary hits **8** and **9** while introduction of aromatic amine functionalities (**17**, **18**) led to loss of potency. Similarly, modification of the 7-position with alkyl chains (**10**, **13**) or oxygen containing ring systems such as furan (**15**, **16**), morpholino (**12**) or oxopyrrolidine

Table 1
Focused library of 7-substituted-1-(3-bromophenylamino)isoquinoline-4-carbonitriles[a]

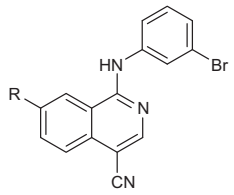

8-18

Compound	R	IC_{50} in μM	
		MLCK	EGFR
8	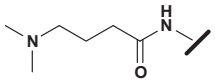	25.1 ± 2.1	4.1 ± 0.6
9	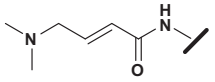	23.6 ± 0.1	0.15 ± 0.1
10	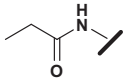	NI	20.8 ± 1.1
11	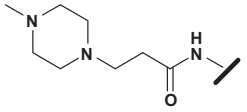	8.7 ± 1.0	1.3 ± 0.4
12	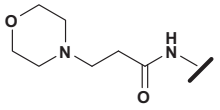	NI	6.9 ± 0.8
13	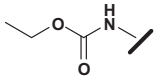	NI	12.8 ± 0.2
14	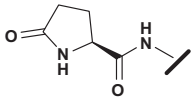	NI	2.2 ± 0.5
15	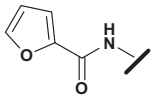	NI	55.6 ± 4.0
16	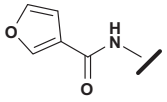	NI	45.2 ± 2.6
17	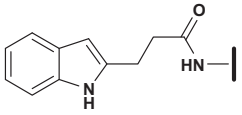	NI	28.0 ± 2.2
18	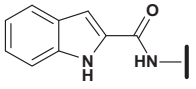	NI	NI

[a] The structures of 7-substituted-1-(3-bromophenylamino)isoquinoline-4-carbonitriles. Compound **9** is an irreversible inhibitor for EGFR. IC_{50} values were measured with an activity-based phosphorylation assay (HTRF) and are presented as an average of at least two independent experiments performed in duplicate. NI indicates 'no inhibition' up to a concentration of 40 μM.

(**14**) was not tolerated by MLCK and no inhibition could be observed up to a concentration of 40 μM. In light of the initial hits **8** and **9** and the newly synthesized derivative **11**, the observed SAR underscores the importance of tertiary amines in the 7-position of the isoquinoline core for MLCK activity and suggests that the protonated tertiary amine may serve as a critical hydrogen bond donor when bound to the target kinase. In order to characterize the mode of inhibition of MLCK by our newly developed isoquinoline in more detail, we performed a Lineweaver–Burk analysis. A double-reciprocal plot of $1/V$ versus 1/[ATP] showed that **11** inhibits MLCK in an ATP-competitive manner, further suggesting that this compound class binds to the ATP pocket of the kinase domain (Fig. 3).

2.4. Biochemical characterization of 11

Being the most potent inhibitor on MLCK in vitro, we then profiled **11** against the same panel of 95 kinases (Fig. 2). Compound **11** inhibited MLCK and CAMK1 potently and revealed a similar profile when compared to **8** and **9**. The two Src kinase family members Lck and YES1, each which possess a Thr gatekeeper, and the serine/threonine specific kinase PHK, which has a large Phe at the gatekeeper position, are also inhibited. The activity of Aurora B (Leu gatekeeper) is moderately inhibited by **11** while the activity of Ca^{2+}/calmodulin dependent kinase CAMKKβ is not perturbed. Unlike in the case of **9**, HER4, PKBβ, FGF-R1 and MKK1 are not strongly inhibited by **11**.

2.5. Modeling 11 to the ATP binding pocket of MLCK

To get deeper insights into the possible binding mode of 7-substituted-1-(3-bromophenylamino)isoquinoline-4-carbonitriles in target kinases and to better understand the preference for kinases with larger or hydrophobic gatekeeper residues, we modeled the most potent inhibitor **11** to the ATP pocket of MLCK (Fig. 4b). Compound **11** is a close structural analog of a class of well known 4-anilino-quinazoline and 4-anilino-quinoline-3-carbonitrile based EGFR and HER2 inhibitors such as erlotinib, gefitinib and EKB-569 and differs by the nitrile in the 4-position of the inhibitor core (Fig. 4a).[20] The crystal structures of various 4-anilino-quinazoline and 4-anilino-quinoline-3-carbonitrile based inhibitors in complex with protein kinases are known from literature and highlight that the N1 nitrogen of the heteroaromatic ring system forms a crucial hydrogen bonding interaction to the backbone of the kinase hinge region.[21] However, such inhibitors were designed to mainly target protein kinases which hold a Thr at the gatekeeper position since the polar side chain of the Thr gatekeeper serves as a hydrogen bond donor and is essential for inhibitor binding and selectivity. In case of **11**, we argue that the nitrile in the 4-position of the inhibitor core would serve as the hydrogen bond acceptor to allow for interactions with the hinge region of the kinase and would position the inhibitor core and the bromo-anilino moiety more distant from the gatekeeper position. This binding mode could explain why the isoquinoline-4-carbonitrile core is well tolerated by larger gatekeeper residues (Leu in MLCK, Phe in PHK and Met in CAMK1). To test this hypothesis, we first generated a homology model of MLCK (family member 1) using the crystal structure of MLCK (family member 4; PDB code: 2X4F) as a template and manually docked compound **11** to the ATP binding site (Fig. 4b). The proposed binding mode of **11** shows the predicted hydrogen bond between the 4-substituted nitrile and the backbone of Val341 of the hinge region. It also reveals a potential charged interaction of the protonated amine of **11** with the side chain of Glu348. We recently observed a similar interaction for (*2E*)-*N*-{4-[(3-bromophenyl)amino]-6-quinazolinyl}-4-(dimethylamino)-2-butenamide in cSrc-S345C.[22] This additional charged interaction could account for the higher potency of **8**, **9** and **11** over **10** and **13** against MLCK. The similar profiles of compounds **8**, **9** and **11** against the selected kinase panel indicates that the selectivity of these compounds is gained from conserved features such as the isoquinoline scaffold together with the presence of the terminal tertiary amino group at the 7-position of the isoquinoline core. Thus, further modifications of **8**, **9** and **11** aided by structure-based

Kinase	Gatekeeper	8	9	11
smMLCK	Leu	11	33	9
PHK	Phe	11	53	38
CAMK1	Met	15	25	14
Lck	Thr	32	60	32
YES1	Thr	36	32	36
Aurora B	Leu	41	33	42
PIM3	Leu	46	59	68
CHK2	Leu	56	51	53
MINK1	Met	59	58	54
IGF-1R	Met	59	73	65
Src	Thr	60	61	49
SYK	Met	64	61	77
BRSK1	Leu	66	95	89
PIM1	Leu	68	73	73
HER4	Thr	69	21	57
PLK1	Leu	69	84	86
DYRK2	Phe	70	68	83
PKCα	Met	70	69	71
p38α MAPK	Thr	71	81	58
SRPK1	Phe	72	55	58
BTK	Thr	72	52	76
DYRK3	Phe	73	75	81
ERK8	Phe	75	78	72
PKD1	Leu	75	79	83
BRSK2	Leu	75	75	100
DYRK1A	Phe	75	60	79
EF2K	Met	78	88	47
AMPK	Met	79	86	77
PAK2	Met	80	81	90
GCK	Met	80	84	84
MELK	Leu	80	75	89
RSK2	Leu	82	87	71
SGK1	Leu	82	82	91
RIPK2	Thr	82	79	66
MNK1	Phe	82	61	95
CHK1	Leu	84	75	68
IKKβ	Met	84	79	88
S6K1	Leu	84	71	82
EPH A2	Thr	84	73	87
RSK1	Leu	84	79	84
PKBβ	Met	85	37	87
MSK1	Leu	86	95	81
NUAK1	Met	86	100	94
MLK1	Met	87	82	91
VEG-FR	Val	87	74	88
CSK	Thr	89	85	81
PAK5	Met	89	86	85
PIM2	Leu	89	69	92

Kinase	Gatekeeper	8	9	11
CAMKKβ	Phe	92	91	87
IR-HIS	Met	93	77	95
HIPK3	Phe	93	91	87
HIPK2	Phe	93	95	88
ERK1	Gln	93	83	85
p38δ MAPK	Met	94	86	77
Aurora A	Leu	94	79	80
PAK4	Met	94	82	86
HIPK1	Phe	95	100	83
TTK	Met	96	74	81
MAPKAP-K3	Met	96	75	91
JNK1	Met	97	91	99
PRK2	Met	98	100	90
JNK2	Met	98	89	100
IRAK4	Tyr	98	93	100
IRR	Met	98	73	86
FGF-R1	Val	99	51	100
MST4	Met	99	81	92
TBK1	Met	99	82	87
MST2	Met	99	82	86
ERK2	Gln	100	81	95
MARK4	Met	100	82	100
MKK1	Met	100	47	79
p38β MAPK	Thr	100	95	100
p38γ MAPK	Met	100	84	100
PDK1	Met	100	97	98
PKBα	Met	100	93	100
PKA	Met	100	100	100
ROCK 2	Met	100	100	100
PKCζ	lieu	100	91	95
MAPKAP-K2	Met	100	97	100
PRAK	Met	100	88	100
GSK3β	Leu	100	78	100
CDK2-Cyclin A	Phe	100	97	100
MARK3	Met	100	96	100
CK1	Met	100	88	100
CK2	Phe	100	99	90
NEK2α	Met	100	98	100
NEK6	Leu	100	81	100
PAK6	Met	100	100	87
EPH-B3	Thr	100	95	90
IKKε	Met	100	80	91
MLK3	Met	100	86	87
LKB1	Met	100	99	100
JNK3	Met	100	83	95
MARK2	Met	100	90	100
MNK2	Phe	100	92	85

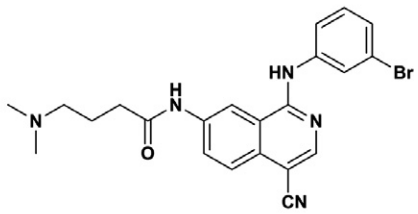

8

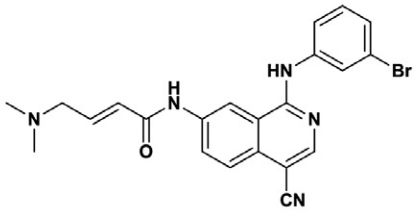

9

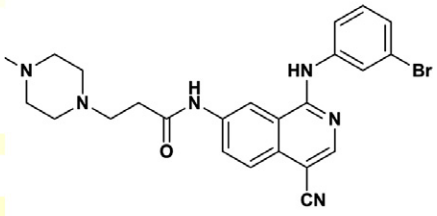

11

Figure 2. Kinase selectivity profiles. Kinase selectivity profiles were determined for **8**, **9** and **11** against a panel of 95 different protein kinases at an inhibitor concentration of 10 μM (National Centre for Protein Kinase Profiling, University of Dundee, UK). The screening was carried out using a radioactive assay. The scores represent the %-activity remaining relative to the 100% DMSO controls. The inhibition is color coded from red (strong inhibition, 0–25% score) to dark yellow (medium inhibition, 25–60% score) to white (weak/no inhibition, >60% score). The size and hydrophobicity of the gatekeeper residue turned out to be an important selectivity filter for this class of compounds.

design may result in even more potent and selective inhibitors active against MLCK.

2.6. Biochemical characterization of compounds and the inhibition of EGFR

An interesting result from the inhibitor profiling outlined above was the observation that **9**, but not its closely related analogs **8** and **11**, is an inhibitor of the receptor tyrosine kinase HER4. The only structural difference between **8** and **9** is the presence of a *trans* double bond (Michael-acceptor) in the *N*,*N*-dimethylamino moiety attached to the 7-position of the inhibitor core. Thus, the difference in HER4 inhibition is likely related to the presence of this Michael acceptor. Members of the HER kinase family such as EGFR (HER1), HER2 and HER4 are known for a conserved cysteine residue that can be targeted by irreversible inhibitors equipped with Michael-acceptors.[23] Cys803 in HER4 is isostructural to Cys797 in EGFR (or Cys773 in an alternative EGFR sequence numbering system) and Cys805 in HER2 and is located at the N-terminal end of a short helix at the lip of the ATP pocket, in which the helix dipole serves to activate the Cys sulfhydryl.[24,25] We hypothesized that the potency of **9** against HER4 might be linked to covalent bond formation of the Michael-acceptor with this unique cysteine residue. Based on this hypothesis, we decided to analyze the effect of **9** on the clinically relevant receptor tyrosine kinase EGFR.

Activating mutations of EGFR are found in 10–20% of patients suffering from non-small cell lung cancer (NSCLC), thus highlighting EGFR as an important target in cancer therapy.[26,27] To investigate the effect of the synthesized 7-substituted 3-bromophenylamino-isoquinoline-4-carbonitriles on the inhibition of EGFR, we carried out phosphorylation assays in the presence and absence of inhibitors (Table 1). Compound **9** was singled out from a set of 11 tested inhibitors and showed nanomolar inhibition of EGFR while all other inhibitors with saturated side chains in the 7-position of the isoquinoline core produced moderate or no inhibition. This finding highlights that the formation of a covalent bond by the Michael-acceptor of **9** is key for potent inhibition of EGFR by the isoquinoline-4-carbonitriles described above.

2.7. Modeling of 9 into the ATP binding pocket of EGFR

In order to understand its possible binding mode, we modeled **9** into the ATP binding pocket of EGFR (Fig. 4c). As described above, isoquinoline-4-carbonitriles can be placed in the ATP binding

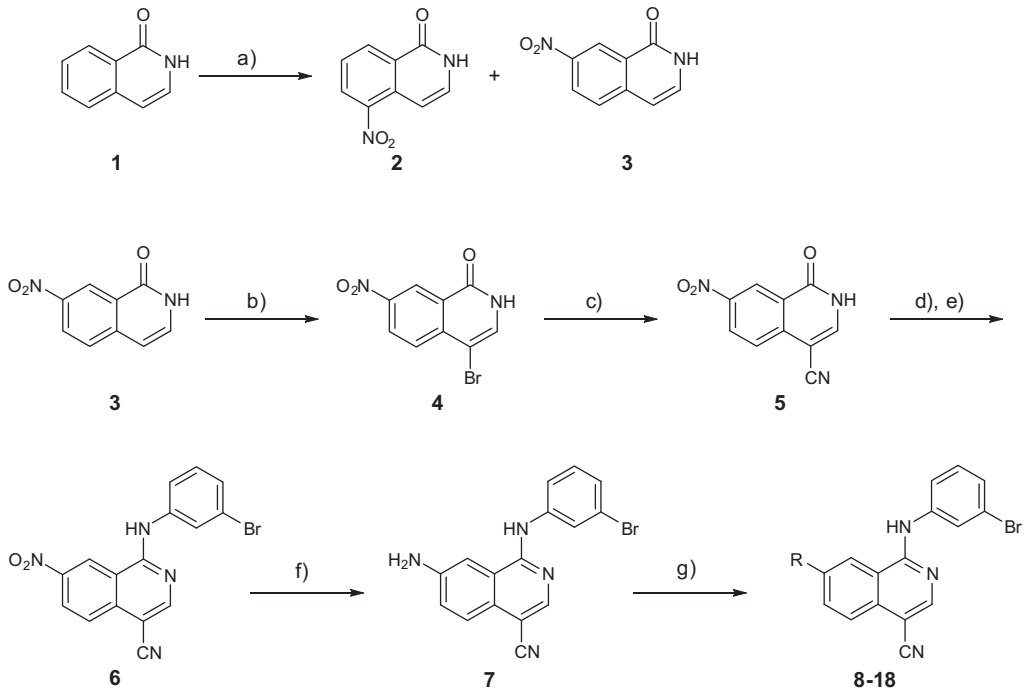

Scheme 1. Synthesis of 7-substituted-1-(3-bromophenylamino)isoquinoline-4-carbonitriles. Reagents and conditions: (a) H_2SO_4, KNO_3; (b) Br_2, DCM; (c) $Zn(CN)_2$, cat. $Pd_2(dba)_3$, cat. S-Phos, DMF/H_2O; (d) $POCl_3$; (e) 3-bromoaniline, pyridine, ethanol; (f) $SnCl_2$, EtOH; (g) acid chloride, Et_3N, THF for **10**, **15**, **16**; acid analog, EDCI·HCl, Et_3N, DMF for **8**; acid analogs, $(COCl)_2$, cat. DMF, THF, Et_3N, for **9**, **11**, **12**, **14**, **17** and **18**.

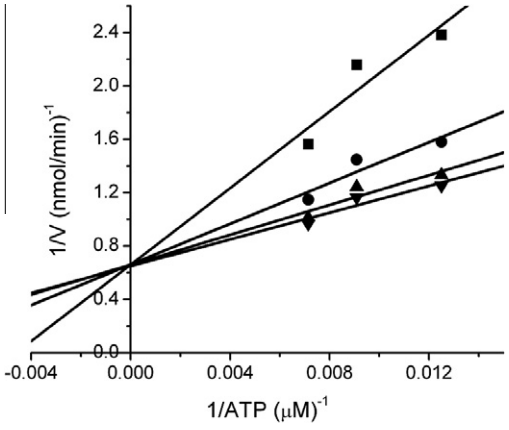

Figure 3. Kinetic analysis of inhibition of MLCK by **11** (Lineweaver-Burk plot). The double reciprocal plot of 1/*V* against 1/[ATP] shows that **11** inhibits MLCK in an ATP-competitive manner. The reaction velocities at 375 nM substrate, three different ATP concentrations (80, 110 and 140 μM) with varying concentrations of **11** (0, 1, 5, 10 μM) were measured and plotted.

pocket of the kinase domain with the nitrile making a key hydrogen bond to the backbone of the hinge region of the kinase domain. When modeled into EGFR, the Michael acceptor of **9** is in close proximity to the conserved cysteine (Cys797), which would allow for covalent bond formation. The observation that **9** is a better EGFR inhibitor than **8** is in line with previously published results which have shown that irreversible inhibitors are generally more potent inhibitors of EGFR than their reversible counterpart.[22,28] The structural model of **9** in complex with EGFR also highlights potential hydrogen bonding interactions of protonated amine functionalities in the 7-position of the inhibitor with the side chain of Asp800 in EGFR (Glu348 in MLCK). We have recently described a similar interaction for 4-anilino-quinazolines when bound to EGFR or the tyrosine kinase cSrc and observed that this interaction significantly increases inhibitor binding.[22,28] In a publication by Wissner et al., two 6,7-dimethoxyisoquinoline-4-carbonitrile analogs were tested and were shown to be very weak inhibitors of EGFR. Based on modeling studies, the authors proposed that the very weak inhibition by 6,7-dimethoxyisoquinoline-4-carbonitriles could be attributed to their inability to form a direct hydrogen bond with backbone atoms in the hinge region of the kinase domain.[29] However, this is at odds with our own modeling studies and in case of **8**, **9** and **11,** we believe that additional potency against EGFR can be gained by the incorporation of a terminal tertiary amine functionality at the 7-position of the isoquinoline core in order to form an extra charged interaction with Asp800 in EGFR. This trend was also observed for MLCK with the exception of **14**, which showed clear preferential activity against EGFR. Interestingly, MLCK has a charged Glu348 side chain at the analogous position of Asp800 of EGFR which is capable of forming the hydrogen bonding interactions described above. Considering this similarity, the discrepancy in potency for **14** against EGFR and MLCK could be the result of two factors. First, the activity-based assays used to study MLCK activity require an additional activator molecule, calmodulin, to attain full MLCK activity, while no such activator is required to measure full EGFR activity. Additionally, it is likely that the flexibility of the various substituents at the 7-position of the isoquinoline core also plays an important role in kinase specificity. In the case of **14**, the substituent is much more rigid when compared to that in **8**, **9** and **11**. However, the carbonyl of the lactam of **14** may also act as a hydrogen bond acceptor. The lack of inhibition observed against MLCK therefore suggests that EGFR can better accommodate the more rigid substituent of **14**.

2.8. Cellular activity of 9

In order to determine cellular activities of the most potent inhibitor **9**, we performed a cell-based screen using 81 genetically defined NSCLC cell lines.[30] The viability of these cells upon inhibitor treatment was determined by measuring the cellular

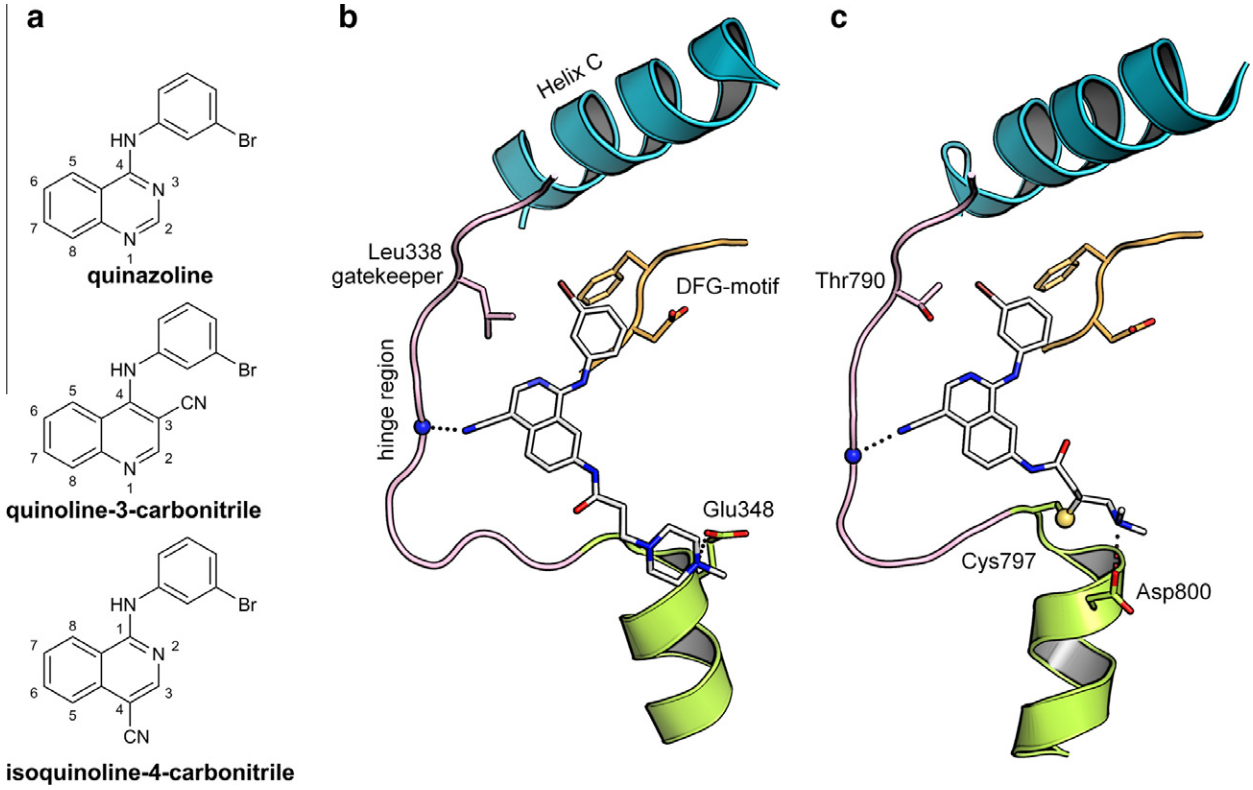

Figure 4. Proposed binding mode of 7-substituted-1-(3-bromophenylamino)isoquinoline-4-carbonitriles to the ATP-binding site of MLCK and EGFR. (a) 4-Anilinoquinazolines and quinoline-3-carbonitrile are known tyrosine kinase inhibitors. Complex crystal structures and detailed SAR studies show that the N1 of the 10-membered ring is crucial for activity and forms a key hydrogen bond to the hinge region of the kinase domain. (b) A structural model of MLCK was generated based on the crystal structure of MLCK family member 4 (PDB code: 2X4F). The proposed binding mode of **11** shows the nitrile of the isoquinoline core within hydrogen bonding distance to the backbone of the hinge region (pink) of the kinase domain. The terminal tertiary amine of the piperazine ring is likely to be protonated under physiological conditions and can be positioned within hydrogen bonding distance to the side chain of Glu348 (black dotted lines). (c) The irreversible inhibitor **9** is modeled to the ATP-binding site of EGFR based on the crystal structure of a 4-anilinoquinazoline bound to EGFR (PDB code: 2J5F). The nitrile of the isoquinoline ring forms a hydrogen bond to the backbone of the hinge region of EGFR and helps to position the electrophile in the 7-position within close proximity to the side chain of Cys797 to allow covalent bond formation. The protonated tertiary amine of the inhibitor side chain forms a charged interaction with the side chain of Asp800, analogous to the type of the extra charged interaction seen in the model for MLCK.

ATP content. The sensitivity profile of **9** shows preferred inhibition of EGFR-mutated and EGFR-dependent cell lines such as PC9 and H3255 (Fig. 5a and b).[30] The viability of cells independent of EGFR signaling such as the KRAS mutant cell line A549 was not inhibited at concentrations up to 40 μM, thus underlining EGFR as the relevant cellular target of **9** (Fig. 5b). A particular challenge in drug development for targeted cancer therapy is the emergence of resistance mutations in EGFR. The T790 M mutation at the gatekeeper position of EGFR is found in nearly 50% of NSCLC patients that relapse from initial treatment with tyrosine kinase inhibitors such as erlotinib or gefitinib.[31] Although irreversible inhibitors of the 4-anilino-quinazoline and -quinoline scaffold were shown to be extremely potent against this EGFR drug resistant mutation in biochemical assays,[20,32] they are only of limited potency in cellular studies and highlight the need for the identification of novel inhibitors.[28] To address this, we evaluated the potency of **9** in the EGFR dependent and drug resistant (EGFR-T790M) NSCLC cell line H1975 and found cellular activity in the high micromolar range (Fig. 5c). This is in accord with our previous findings where we analyzed the determinants of the activity and selectivity of clinically relevant reversible and irreversible 4-anilino-quinazoline and -quinoline based EGFR inhibitors by chemogenomic profiling against genetically defined NSCLC cell lines.[28] Although our modeling studies suggest that the nitrile pushes the inhibitor scaffold away from the gatekeeper to avoid a steric clash with larger amino acid side chains, it is likely that M790 in EGFR-T790M still interferes sterically with the binding of **11**. These effects would also affect the reversible binding of **9** to EGFR-T790M, thereby explaining the weak activity of **9** in H1975 cells which harbor this mutation. Along these lines, we recently showed that both steric hindrance of the initial reversible binding combined with increased competition with ATP act in concert and transmit drug-resistance at least for 4-anilino-quinazolines in EGFR-T790M.[25]

3. Conclusion

7-Substituted-1-(3-bromophenylamino)isoquinoline-4-carbonitriles represent an interesting class of novel kinase inhibitors with a preference for MLCK and EGFR. We have synthesized 7-substituted-1-(3-bromophenylamino)isoquinoline-4-carbonitrile derivatives and evaluated their activities against MLCK using in vitro kinase assays and showed that inhibition of the phosphorylation reaction depends on the nature of the substituent at the 7-position of the isoquinoline scaffold. The presence of a terminal tertiary amine moiety at this position was found to be required for biological activity. The preference of the compounds for inhibiting kinases which possess a bulky hydrophobic amino acid residue at the gatekeeper position was explained by modeling **11** into the ATP binding pocket of MLCK. Guided by biochemical profiling, we identified the irreversible isoquinoline-4-carbonitrile **9** as a potent inhibitor of HER-kinases with low micromolar cellular activity. Modeling studies suggest that the electrophile of **9** alkylates a Cys residue at the lip of these ATP pocket known to be sensitive for covalent inactivation by irreversible 4-anilino-

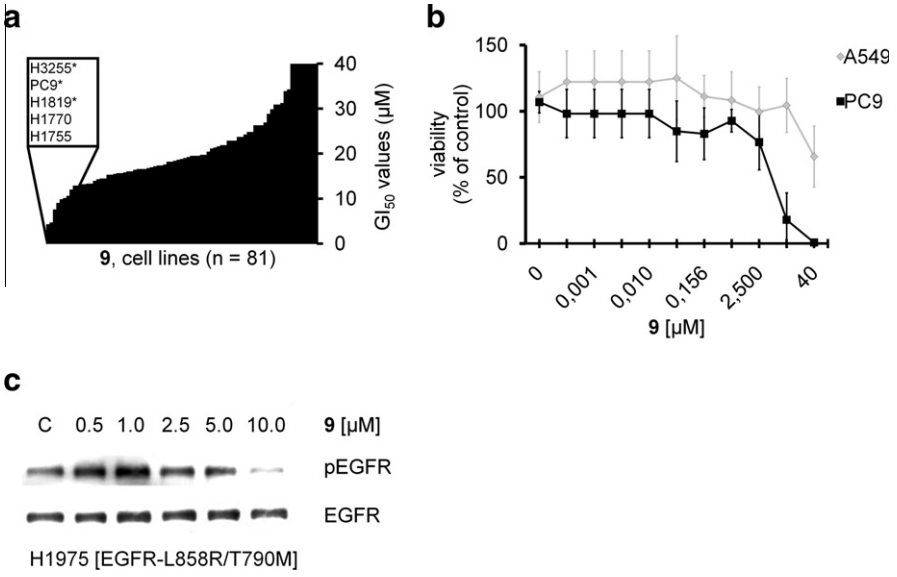

Figure 5. Growth inhibition of NSCLC cell lines by **9**. (a) The cellular activity profile of **9** is depicted in a chart presentation where GI_{50} values are plotted against genetically annotated NSCLC cell lines.[28,30] Cells were treated with various concentrations of compound and cell viability was determined by measuring the cellular ATP content. The five most sensitive cell lines are highlighted and EGFR/HER2 dependent or mutated cell lines are marked by an asterisk. (b) EGFR mutant NSCLC cell line PC9 and the KRAS mutant cell line A549 (negative control since independent of EGFR) were treated with increasing concentrations of **9** and the viability of the cells was again determined by measuring the cellular ATP content. The error bars represent the standard deviation for three replicates. (c) The drug resistant NSCLC cell line H1975 expressing the EGFR-T790M gatekeeper mutant was treated with increasing concentrations of **9** and showed only limited inhibition. Inhibition of the activation status of mutant EGFR was determined by immunoblotting and measuring levels of phosphorylated EGFR.

quinazolines and -quinolines. In light of these biochemical and biological observations, we feel that the discussed isoquinoline-4-carbonitriles may serve as valuable starting points for further compound design to generate probe molecules which allow for the investigation of kinase biology in chemical biology research.

4. Experimental

4.1. Synthesis of compounds

^1H and ^{13}C NMR spectra were recorded on a Varian Mercury 400, Bruker DRX 500 or Varian Inova 600 spectrometer. The spectra refer to the residual solvent signals: dimethylsulfoxide-d_6 (2.50 ppm) for ^1H and (39.52 ppm) for ^{13}C. Chemical shifts (δ) are given in parts per million (ppm) while the coupling constants (J) are reported in hertz (Hz). The following abbreviations are used; s = singlet, d = doublet, dd = doublet of doublet, ddd = doublet of doublet of doublet, t = triplet, td = triplet of doublet, dt = doublet of triplet, q = quartet, qd = quartet of doublet, qn = quintet, br s = broad singlet, m = multiplet. LC–MS spectra were obtained on a LTQ Orbitrap (high resolution mass spectrometer from Thermo Electron) coupled to an 'Accela' HPLC System (consisting of Accela pump, Accela autosampler and Accela PDA detector) supplied with a 'Hypersil GOLD' column (50 mm × 1 mm, 1.9 μm particle size) from Thermo Electron. Analytical TLC was carried out on Merck 60 F_{245} aluminium-backed silica gel plates. Compounds were purified by column chromatography using Baker silica gel (40–70 μm particle size). Preparative HPLC was carried out on the final compounds using a Varian Prostar with UV-detector (Model 340) and a VP 25-21 Nucleodur (C18 Gravity, 5 μ) column (Serial No. 2105150). Anhydrous solvents were purchased from Acros Organics and Fluka. Other chemical materials were purchased from Alfa Aesar, Fluka, and Sigma–Aldrich and were used as received.

4.1.1. 7-Nitroisoquinoline-1(2*H*)-one (3)

1-Isoquinolinol (4.0 g, 6.89 mmol) was added portionwise in ice-cooled sulfuric acid (25 mL). Once the solid was dissolved, KNO_3 (3.4 g, 33.62 mmol) was added in portions and the reaction mixture was stirred at 0 °C for 30 min. The mixture was then allowed to warm to room temperature and was stirred overnight. The next day, the reaction mixture was poured on ice and the resulted suspension was extracted three times with chloroform. The organic phases were combined, dried with sodium sulfate and evaporated under vacuum. The obtained viscous liquid was repeatedly purified by column chromatography (EtOAc/petroleum ether, 0.25:0.75 to 1:0) to furnish two positional isomers as yellow crystalline material, 1.06 g (20%) of 5-nitroisoquinoline-1(2*H*)-one, **2**, and 710 mg (14%) of the required 7-nitro isomer **3**. The analytical data for **3**: ^1H NMR (400 MHz, DMSO-d_6): 11.74 (br s, 1H), 8.89 (d, J = 2.6 Hz, 1H), 8.43 (dd, J = 8.8, 2.6 Hz, 1H), 7.90 (d, J = 8.8 Hz, 1H), 7.45 (d, J = 7.1 Hz, 1H), 6.72 (d, J = 7.1 Hz, 1H); ^{13}C NMR (101 MHz, DMSO-d_6): 161.13, 145.07, 142.81, 133.47, 128.09, 126.14, 125.66, 122.62, 104.06; HRMS (ESI-MS): Calcd for $C_9H_7N_3O_3$ [M+H$^+$]: 191.04512. Found: 191.04501. The analysis for **2**: ^1H NMR (500 MHz, DMSO-d_6): 11.73 (br s, 1H), 8.56 (d, J = 8.0 Hz, 1H), 8.44 (d, J = 8.0 Hz, 1H), 7.64 (t, J = 8.0 Hz, 1H), 7.42–7.47 (m, 1H), 6.95 (d, J = 7.6 Hz, 1H); ^{13}C NMR (126 MHz, DMSO-d_6): 160.35, 144.51, 133.18, 133.11, 130.93, 129.34, 127.75, 125.71, 98.47; HRMS (ESI-MS): Calcd for $C_9H_7N_3O_3$ [M+H$^+$]: 191.04512. Found:191.04509.

4.1.2. 4-Bromo-7-nitroisoquinolin-1(2*H*)-one (4)

Compound **3** (1.49 g, 7.84 mmol) was dissolved in DCM (25 mL) and bromine (0.44 mL, 8.56 mmol) was added. The reaction mixture was stirred at room temperature. After 5 h, the reaction was stopped and the solvent was evaporated under reduced pressure. The mixture was column chromatographed (EtOAc/petroleum ether, 1:1) to produce 1.3 g (62%) of **4** as a yellow solid. ^1H NMR (400 MHz, DMSO-d_6): 12.06 (br s, 1H), 8.85 (d, J = 2.4 Hz, 1H), 8.53 (dd, J = 9.0, 2.4 Hz, 1H), 7.91 (d, J = 9.0 Hz, 1H), 7.81 (s, 1H); ^{13}C NMR (101 MHz, DMSO-d_6): 160.16, 145.65, 140.24, 134.46, 127.31, 127.17, 126.24, 122.87, 96.25; HRMS (ESI-MS): Calcd for $C_9H_6{}^{79}BrN_2O_3$ [M+H$^+$]: 268.95563, for $C_9H_6{}^{81}BrN_2O_3$ [M+H$^+$]: 270.95358. Found: 268.95599, 270.95357.

4.1.3. 7-Nitro-1-oxo-1,2-dihydroisoquinoline-4-carbonitrile (5)

4-Bromo-7-nitroisoquinolin-1(2*H*)-one **4** (1.2 g, 4.4 mmol), $Pd_2(dba)_3$ (0.34 g, 0.37 mmol), S-Phos (0.34 g, 0.83 mmol) and $Zn(CN)_2$ (0.63 g, 5.36 mmol) were suspended in DMF/H_2O (32 mL, 99:1 v/v). The reaction mixture was degassed for 20 min, heated at 140 °C for 20 min. The temperature of the reaction mixture was lowered to 120 °C and stirring was continued for an additional 3 h. The progress of the reaction was monitored by TLC. Once completed, the mixture was diluted with water and extracted with EtOAc (3 × 400 mL). The combined EtOAc layers were dried over sodium sulfate, filtered and concentrated under vacuum. The resulting crude was purified by column chromatography (EtOAc/petroleum ether, 0.3:0.7 to 0.6:0.4) to obtain 476 mg (49%) of **5** as yellow crystalline material. ^{1}H NMR (400 MHz, DMSO-d_6): 12.65 (br s, 1H), 8.89 (d, J = 2.5 Hz, 1H), 8.62 (dd, J = 8.8, 2.5 Hz, 1H), 8.46 (s, 1H), 7.94 (d, J = 8.8 Hz, 1H); ^{13}C NMR (101 MHz, DMSO-d_6): 160.31, 146.11, 143.57, 138.94, 127.77, 125.48, 125.09, 122.84, 115.50, 87.85; HRMS (ESI-MS): Calcd for $C_{10}H_6N_3O_3$ [M+H$^+$]: 216.04037. Found: 216.04049.

4.1.4. 1-(3-Bromophenylamino)-7-nitroisoquinoline-4-carbonitrile (6)

The 7-nitro-1-oxo-1,2-dihydroisoquinoline-4-carbonitrile **5** (470 mg, 2.18 mmol) was added to $POCl_3$ (25 mL) and refluxed for 5 h. The excess of $POCl_3$ was removed under reduced pressure and the resulting crude intermediate, 1-chloro-7-nitro-1,2-dihydroisoquinoline-4-carbonitrile, was thoroughly dried under high vacuum. The next day, the crude intermediate along with 3-bromoaniline (260 μL, 2.40 mmol) and pyridine (0.21 mL, 2.57 mmol) was refluxed in ethanol for 2.5 h. The solvent was removed under vacuum and the resulting crude was column chromatographed using EtOAc/petroleum ether (0:1 to 1:1) to obtain 460 mg (58%) of **6** as a yellow solid. ^{1}H NMR (400 MHz, DMSO-d_6): 10.55 (br s, 1H), 9.72 (d, J = 2.1 Hz, 1H), 8.74 (s, 1H), 8.64 (dd, J = 9.1, 2.2 Hz, 1H), 8.08–8.13(m, 2H), 7.85 (dt, J = 7.0, 2.2 Hz, 1H), 7.43–7.34 (m, 2H); ^{13}C NMR (151 MHz, DMSO-d_6): 156.11, 152.39, 146.12, 140.36, 138.64, 130.49, 127.00, 126.18, 125.76, 125.04, 121.55, 121.49, 121.18, 116.85, 116.40, 94.90; HRMS (ESI-MS): Calcd for $C_{16}H_{10}{}^{79}BrN_4O_2$ [M+H$^+$]: 368.99816, for $C_{16}H_{10}{}^{81}BrN_4O_2$ [M+H$^+$]: 370.99612. Found: 368.99862, 370.99617.

4.1.5. 7-Amino-1-(3-bromophenylamino)isoquinoline-4-carbonitrile (7)

1-(3-Bromophenylamino)-7-nitroisoquinoline-4-carbonitrile **6** (300 mg, 0.82 mmol) and tin(II) chloride (900 mg, 4.74 mmol) were added in ethanol (60 mL) and heated at 70 °C for 3 h. Upon completion, the reaction mixture was concentrated to 10 mL and added to saturated aq $NaHCO_3$ (20 mL). The aqueous layer was extracted with EtOAc (3 × 100 mL) and dried over sodium sulfate, filtered and concentrated under vacuum to obtain a crude product which was purified by column chromatography (EtOAc/petroleum ether, 0.2:0.8 to 0.4:0.6) to furnish 240 mg (87%) of **7** as a yellow solid. ^{1}H NMR (400 MHz, DMSO-d_6): 9.55 (s, 1H), 8.23 (s, 1H), 8.12 (t, J = 1.8 Hz, 1H), 7.81 (dd, J = 8.2, 0.9 Hz, 1H), 7.67 (d, J = 8.8 Hz, 1H), 7.47 (d, J = 1.8 Hz, 1H), 7.27–7.36 (m, 2H), 7.20–7.25 (m, 1H), 5.88 (br s, 2H); ^{13}C NMR (101 MHz, DMSO-d_6): 153.10, 149.04, 143.20, 141.93, 130.28, 126.01, 125.18, 124.71, 123.48, 123.04, 121.18, 120.14, 119.53, 117.96, 102.70, 95.92; HRMS (ESI-MS): Calcd for $C_{16}H_{12}{}^{79}BrN_4$ [M+H$^+$]: 339.02399, for $C_{16}H_{12}{}^{81}BrN_4$ [M+H$^+$]: 341.02194. Found: 339.02437, 341.02175.

4.1.6. *N*-(1-(3-Bromophenylamino)-4-cyanoisoquinolin-7-yl)-4-(dimethylamino)butanamide (8)

4-(Dimethylamino)butanoic acid hydrochloride (20 mg, 0.12 mmol) and EDCI·HCl (22 mg, 0.12 mmol) were added to 1 mL of dry DMF followed by triethylamine (34 μL, 0.24 mmol) and stirred at 0 °C for 30 min. 7-Amino-1-(3-bromophenylamino)isoquinoline-4-carbonitrile **7** (20 mg, 0.059 mmol) was added into the reaction mixture and the resulting mixture was stirred at room temperature for 48 h, subsequently added to aq $NaHCO_3$, extracted with EtOAc (3 × 100 mL), concentrated under vacuum and column chromatographed (MeOH/DCM with triethylamine, 0:1 to 0.15:0.85) to obtain a yellowish powder which was further purified by preparative HPLC affording 20 mg (74%) of **8** as an off-white powder. ^{1}H NMR (400 MHz, DMSO-d_6): 10.45 (s, 1H), 9.95 (s, 1H), 8.85 (s, 1H), 8.47 (s, 1H), 8.07 (s, 1H), 7.99 (dd, J = 8.8, 1.5 Hz, 1H), 7.90 (d, J = 8.8 Hz, 1H), 7.79 (d, J = 8.0 Hz, 1H), 7.33 (t, J = 8.0 Hz, 1H), 7.28 (d, J = 8.0 Hz, 1H), 2.44 (t, J = 7.4 Hz, 2H), 2.34 (t, J = 7.1 Hz, 2H), 2.20 (s, 6H), 1.79 (qn, J = 7.3 Hz, 2H); ^{13}C NMR (101 MHz, DMSO-d_6): 171.52, 154.71, 147.07, 141.50, 138.78, 130.98, 130.32, 126.46, 125.82, 124.37, 124.23, 121.15, 120.86, 118.03, 117.55, 112.87, 95.47, 58.19, 44.80 (C × 2), 33.96, 22.56; HRMS (ESI-MS): Calcd for $C_{22}H_{23}{}^{79}BrN_5O$ [M+H$^+$]: 452.10805, for $C_{22}H_{23}{}^{81}BrN_5O$ [M+H$^+$]: 454.10600. Found: 452.10771, 454.10543.

4.1.7. (*E*)-*N*-(1-(3-Bromophenylamino)-4-cyanoisoquinolin-7-yl)-4-(dimethylamino)but-2-enamide (9)

(*E*)-4-(Dimethylamino)but-2-enoic acid hydrochloride (39 mg, 0.235 mmol) was added to 1.5 mL DCM and cooled to 0 °C under argon. Oxalyl chloride (21 μL, 0.240 mmol) was added dropwise followed by a catalytic amount of DMF. The reaction mixture was stirred at 30 °C for 2 h (solution A). 7-Amino-1-(3-bromophenylamino)isoquinoline-4-carbonitrile **7** (20 mg, 0.059 mmol) was dissolved in 1-methyl-2-pyrrolidinone (0.2 mL) and added to pre-cooled solution A. The reaction mixture was stirred for 1.5 h at room temperature and then poured into saturated aq $NaHCO_3$, extracted with EtOAc (3 × 100 mL), washed with brine and concentrated under high vacuum. The crude product was purified by preparative HPLC to obtain 8 mg (31%) of **9** as a yellow solid. ^{1}H NMR (400 MHz, DMSO-d_6): 10.59 (s, 1H), 10.00 (s, 1H), 8.95 (s, 1H), 8.49 (s, 1H), 8.06 (s, 1H), 7.99 (dd, J = 8.9, 1.5 Hz, 1H), 7.93 (d, J = 8.8 Hz, 1H), 7.79 (d, J = 8.2 Hz, 1H), 7.34 (t, J = 8.0 Hz, 1H), 7.28 (d, J = 8.1 Hz, 1H), 6.84 (dt, J = 15.4, 6.0 Hz, 1H), 6.38 (d, J = 15.4 Hz, 1H), 3.18 (d, J = 5.6 Hz, 2H), 2.25 (s, 6H); ^{13}C NMR (101 MHz, DMSO-d_6): 163.45, 154.73, 147.27, 141.46, 138.55, 131.23, 130.36, 126.47, 125.99, 125.88, 124.51, 124.22, 121.17, 120.84, 117.99, 117.53, 113.30, 95.49, 59.48, 44.91 (C × 2); HRMS (ESI-MS): Calcd for $C_{22}H_{21}{}^{79}BrN_5O$ [M+H$^+$]: 450.09240, for $C_{22}H_{21}{}^{81}BrN_5O$ [M+H$^+$]: 452.08999. Found: 450.09210, 452.08999.

4.1.8. *N*-(1-(3-Bromophenylamino)-4-cyanoisoquinolin-7-yl)propionamide (10)

Propionyl chloride (5.7 μL, 0.065 mmol), 7-amino-1-(3-bromophenylamino)isoquinoline-4-carbonitrile **7** (20 mg, 0.059 mmol) and triethylamine (18 μL, 0.130 mmol) were added to 1 mL of THF at room temperature. After 2 h of stirring, the reaction mixture was poured into aq. $NaHCO_3$, extracted with EtOAc, washed with brine and dried over sodium sulfate. The crude compound was dissolved in a minimum amount of acetone and a few drops of petroleum ether were added. The mixture was concentrated under reduced pressure to produce a suspension. The suspended solid was allowed to settle down and the liquid was decanted. The solid was further washed with petroleum ether and dried to obtain 10 mg (43%) of **10** as an off-white solid. ^{1}H NMR (400 MHz, DMSO-d_6): 10.33 (s, 1H), 9.94 (s, 1H), 8.84 (s, 1H), 8.47 (s, 1H), 8.06 (t, J = 1.8 Hz, 1H), 7.98–7.87 (m, 2H), 7.80–7.75 (m, 1H), 7.33 (t, J = 7.8 Hz, 1H), 7.30–7.25 (m, 1H), 2.43 (q, J = 7.5 Hz, 2H), 1.15 (t, J = 7.5 Hz, 3H); ^{13}C NMR (101 MHz, DMSO-d_6): 172.33, 154.66, 147.00, 141.45, 138.72, 130.95, 130.27, 126.39, 125.78, 124.34, 124.20, 121.10, 120.81, 117.98, 117.46, 112.86, 95.46, 29.39, 9.49; HRMS (ESI-MS): Calcd for $C_{19}H_{16}{}^{79}BrN_4O$ [M+H$^+$]: 395.05020, for $C_{19}H_{16}{}^{81}BrN_4O$ [M+H$^+$]: 397.04815. Found: 395.05001, 397.04779.

4.1.9. *N*-(1-(3-Bromophenylamino)-4-cyanoisoquinolin-7-yl)-3-(4-methylpiperazin-1yl)propanamide (11)

3-(4-Methylpiperazin-1-yl)propanoic acid (38 mg, 0.220 mmol) was added in 2 mL THF and cooled to 0 °C under argon. Oxalyl chloride (20 μL, 0.228 mmol) was added dropwise followed by a drop of DMF. The reaction mixture was stirred at 40 °C for 3 h (solution A). 7-Amino-1-(3-bromophenylamino)isoquinoline-4-carbonitrile **7** (25 mg, 0.073 mmol) was dissolved in 1-methyl-2-pyrrolidinone (0.5 mL) and added to pre-cooled solution A. The reaction mixture was stirred overnight at room temperature and then poured into saturated aq $NaHCO_3$ solution, extracted with EtOAc (3 × 100 mL), washed with brine and concentrated under high vacuum. The crude product was first purified by column chromatography (MeOH/DCM, 0:1 to 0.1:0.9) to obtain a hygroscopic compound which was further purified by preparative HPLC to yield 14 mg (39%) of **11** as an off-white powder. ^{1}H NMR (400 MHz, DMSO-d_6): 10.56 (s, 1H), 9.99 (s, 1H), 8.83 (s, 1H), 8.48 (s, 1H), 8.06 (t, J = 1.7 Hz, 1H), 7.99 (dd, J = 8.9, 1.4 Hz, 1H), 7.92 (d, J = 8.8 Hz, 1H), 7.78 (d, J = 8.2 Hz, 1H), 7.33 (t, J = 8.0 Hz, 1H), 7.30–7.26 (m, 1H), 2.68 (t, J = 6.8 Hz, 2H), 2.57 (t, J = 6.8 Hz, 2H), 2.50–2.34 (m, 8H), 2.21 (s, 3H); ^{13}C NMR (101 MHz, DMSO-d_6): 170.60, 154.72, 147.13, 141.50, 138.70, 131.05, 130.35, 126.29, 125.85, 124.50, 124.23, 121.17, 120.85, 118.04, 117.55, 112.76, 95.48, 54.48 (C × 2), 53.57, 52.10 (C × 2), 45.36, 34.03; HRMS (ESI-MS): Calcd for $C_{24}H_{26}{}^{79}BrN_6O$ [M+H$^+$]: 493.13460, for $C_{24}H_{26}{}^{81}BrN_6O$ [M+H$^+$]: 495.13255. Found: 493.13409, 495.13197.

4.1.10. *N*-(1-(3-Bromophenylamino)-4-cyanoisoquinolin-7-yl)-3-morpholinopropanamide (12)

From 3-morpholinopropanoic acid hydrochloride (46 mg, 0.235 mmol), oxalyl chloride (21 μL, 0.240 mmol), catalytic DMF was dissolved in 1 mL DCM and heated for 2 h at 30 °C. 7-Amino-1-(3-bromophenylamino)isoquinoline-4-carbonitrile **7** (20 mg, 0.059 mmol in 0.2 mL of 1-methyl-2-pyrrolidinone) was added and stirred at room temperature for 2 h as described in the procedure for **9**. The crude product was purified by preparative HPLC, producing 11 mg (39%) of **12** as a white solid. ^{1}H NMR (400 MHz, DMSO-d_6): 10.52 (br s, 1H), 9.99 (br s, 1H), 8.83 (s, 1H), 8.48 (s, 1H), 8.06 (t, J = 1.7 Hz, 1H), 7.99 (dd, J = 8.9, 1.5 Hz, 1H), 7.92 (d, J = 8.8 Hz, 1H), 7.78 (d, J = 8.2 Hz, 1H), 7.34 (t, J = 8.0 Hz, 1H), 7.28 (d, J = 8.2 Hz, 1H), 3.58 (t, J = 4.4 Hz, 4H), 2.68 (t, J = 6.7, Hz, 2H), 2.59 (t, J = 6.7 Hz, 2H), 2.47–2.38 (m, 4H); ^{13}C NMR (151 MHz, DMSO-d_6): 170.51, 154.73, 147.06, 141.46, 138.64, 131.03, 130.29, 126.31, 125.81, 124.42, 124.22, 121.11, 120.83, 118.00, 117.46, 112.79, 95.45, 66.14 (C × 2), 54.05, 53.05 (C × 2), 33.77; HRMS (ESI-MS): Calcd for $C_{23}H_{23}{}^{79}BrN_5O_2$ [M+H$^+$]: 480.10296, for $C_{23}H_{23}{}^{81}BrN_5O_2$ [M+H$^+$]: 482.10092. Found: 480.10257, 482.10048.

4.1.11. Ethyl 1-(3-Bromopheylamino)-4-cyanoisoquinolin-7-ylcarbamate (13)

7-Amino-1-(3-bromophenylamino)isoquinoline-4-carbonitrile **7** (10 mg, 0.030 mmol), ethyl chloroformate (3.37 μL, 0.035 mmol) and triethylamine (9 μL, 0.065 mmol) were added to pre-cooled THF. The reaction mixture was stirred at room temperature for 6 days. Upon completion, the reaction mixture was concentrated and purified by preparative HPLC to obtain 6 mg (50%) of **13** as a white solid. ^{1}H NMR (400 MHz, DMSO-d_6): 10.13 (s, 1H), 9.95 (br s, 1H), 8.68 (s, 1H), 8.46 (s, 1H), 8.05 (s, 1H), 7.90–7.86 (m, 2H), 7.77 (d, J = 7.7 Hz, 1H), 7.33 (t, J = 8.0 Hz, 1H), 7.30–7.25 (m, 1H), 4.21 (q, J = 7.1 Hz, 2H), 1.29 (t, J = 7.1 Hz, 3H); ^{13}C NMR (101 MHz, DMSO-d_6): 154.57, 153.73, 146.92, 141.50, 138.95, 138.83, 130.63, 130.34, 125.82, 124.48, 124.18, 121.16, 120.87, 118.13, 117.53, 111.73, 95.42, 60.63, 14.56; HRMS (ESI-MS): Calcd for $C_{19}H_{16}{}^{79}BrN_4O_2$ [M+H$^+$]: 411.04511, for $C_{19}H_{16}{}^{81}BrN_4O_2$ [M+H$^+$]: 413.04307. Found: 411.04492, 413.04236.

4.1.12. (*S*)-*N*-(1-(3-Bromophenylamino)-4-cyanoisoquinolin-7-yl)-5-oxopyrrolidine-2-carboxamide (14)

From L-pyroglutamic acid (30 mg, 0.232 mmol), oxalyl chloride (20.70 μL, 0.236 mmol), catalytic DMF in was dissolved in 1.5 mL DCM and stirred for 2 h at 30 °C. 7-Amino-1-(3-bromophenylamino)isoquinoline-4-carbonitrile **7** (20 mg, 0.059 mmol in 0.2 mL of 1-methyl-2-pyrrolidinone) was added and stirred for 2 h at room temperature as described for **9**. Preparative HPLC on the crude product produced 7 mg (27%) of **14** as an off-white solid. ^{1}H NMR (400 MHz, DMSO-d_6): 10.56 (s, 1H), 10.03 (s, 1H), 8.86 (s, 1H), 8.49 (s, 1H), 8.11–7.98 (m, 3H), 7.94 (d, J = 8.9 Hz, 1H), 7.77 (d, J = 7.9 Hz, 1H), 7.34 (t, J = 7.9 Hz, 1H), 7.28 (d, J = 8.0 Hz, 1H), 4.30 (dd, J = 8.3, 3.8 Hz, 1H), 2.46–2.35 (m, 1H), 2.31–2.14 (m, 2H), 2.13–2.03 (m, 1H); ^{13}C NMR (101 MHz, DMSO-d_6): 177.51, 171.85, 154.77, 147.38, 141.42, 138.26, 131.36, 130.36, 126.50, 125.95, 124.60, 124.35, 121.16, 120.97, 117.95, 117.52, 113.32, 95.45, 56.38, 29.24, 25.34; HRMS (ESI-MS): Calcd for $C_{21}H_{17}{}^{79}BrN_5O_2$ [M+H$^+$]: 450.05601, for $C_{21}H_{17}{}^{81}BrN_5O_2$ [M+H$^+$]: 452.05397. Found: 450.05572, 452.05360.

4.1.13. *N*-(1-(3-Bromophenylamino)-4-cyanoisoquinolin-7-yl)furan-2-carboxamide (15)

7-Amino-1-(3-bromophenylamino)isoquinoline-4-carbonitrile **7** (20 mg, 0.059 mmol), furan-2-carboxylic acid chloride (6.2 μL, 0.064 mmol) and triethylamine (18 μL, 0.128 mmol) in 2 mL THF were stirred at 0 °C for 30 min. The reaction mixture was concentrated and the crude product was purified by preparative HPLC to obtain 8 mg (32%) of **15** as an off-white solid. ^{1}H NMR (400 MHz, DMSO-d_6): 10.72 (br s, 1H), 10.03 (br s, 1H), 8.98 (s, 1H), 8.51 (s, 1H), 8.19 (dd, J = 8.8, 1.5 Hz, 1H), 8.13–7.98 (m, 2H), 7.94 (d, J = 8.9 Hz, 1H), 7.81 (d, J = 8.0 Hz, 1H), 7.48 (d, J = 3.3 Hz, 1H), 7.32 (t, J = 8.0 Hz, 1H), 7.29-7.24 (m, 1H), 6.73 (m, 1H); ^{13}C NMR (101 MHz, DMSO-d_6): 156.43, 154.71, 147.50, 147.13, 146.27, 141.40, 137.95, 131.44, 130.34, 127.47, 125.89, 124.31, 124.19, 121.18, 120.80, 117.81, 117.53, 115.38, 114.85, 112.34, 95.43; HRMS (ESI-MS): Calcd for $C_{21}H_{14}{}^{79}BrN_4O_2$ [M+H$^+$]: 433.02946, for $C_{21}H_{14}{}^{81}BrN_4O_2$ [M+H$^+$]: 435.02742. Found: 433.02933, 435.02715.

4.1.14. *N*-(1-(3-Bromophenylamino)-4-cyanoisoquinolin-7-yl)furan-3-carboxamide (16)

7-Amino-1-(3-bromophenylamino)isoquinoline-4-carbonitrile **7** (20 mg, 0.059 mmol), furan-3-carboxylic acid chloride (8.4 mg, 0.064 mmol) and triethylamine (18 μL, 0.128 mmol) were added to THF at room temperature and the reaction mixture was stirred for 30 min. The solvent was evaporated under high vacuum and the crude was purified by preparative HPLC and crystallization, furnishing 7 mg (28%) of **16** as a brown solid. ^{1}H NMR (400 MHz, DMSO-d_6): 10.52 (br s, 1H), 10.02 (br s, 1H), 8.97 (s, 1H), 8.54–8.49 (m, 2H), 8.21 (dd, J = 8.8, 1.7 Hz, 1H), 8.13 (t, J = 1.9 Hz, 1H), 7.96 (d, J = 8.9 Hz, 1H), 7.88–7.82 (m, 2H), 7.34 (t, J = 8.0 Hz, 1H), 7.30–7.26 (m, 1H), 7.09 (s, 1H); ^{13}C NMR (101 MHz, DMSO-d_6): 160.63, 154.67, 147.35, 146.26, 144.48, 141.41, 138.36, 131.27, 130.34, 127.20, 125.83, 124.33, 124.11, 122.61, 121.15, 120.67, 117.85, 117.47, 114.40, 109.13, 95.41; HRMS (ESI-MS): Calcd for $C_{21}H_{14}{}^{79}BrN_4O_2$ [M+H$^+$]: 433.02946, for $C_{21}H_{14}{}^{81}BrN_4O_2$ [M+H$^+$]: 435.02742. Found: 433.02921, 435.02702.

4.1.15. *N*-(1-(3-Bromophenylamino)-4-cyanoisoquinolin-7-yl)-3-(1*H*-indol-3-yl)propanamide (17)

Indole-3-propionic acid (44 mg, 0.232 mmol), oxalyl chloride (20.7 μL, 0.236 mmol), catalytic DMF in 1 mL DCM was stirred for 2 h at 30 °C before and 7-amino-1-(3-bromophenylamino)isoquinoline-4-carbonitrile **7** (20 mg, 0.059 mmol in 0.2 mL of 1-methyl-2-pyrrolidinone) as added and stirred for additional 2 h at room temperature as described in the procedure for **9**. Column chromatography of the crude product (EtOAc/petroleum ether, 0.1:0.9 to

0.6:0.4) resulted in 8 mg (27%) of **17** as a viscous liquid. ^{1}H NMR (400 MHz, DMSO-d_6) 10.81 (s, 1H), 10.44 (s, 1H), 9.99 (s, 1H), 8.85 (s, 1H), 8.48 (s, 1H), 8.06 (t, J = 1.8 Hz, 1H), 7.98 (dd, J = 8.9, 1.6 Hz, 1H), 7.91 (d, J = 8.8 Hz, 1H), 7.77 (d, J = 8.1 Hz, 1H), 7.59 (d, J = 7.8 Hz, 1H), 7.33 (t, J = 7.7 Hz, 2H), 7.28 (d, J = 8.0 Hz, 1H), 7.18 (d, J = 1.6 Hz, 1H), 7.07 (t, J = 7.1 Hz, 1H), 6.99 (t, J = 7.3 Hz, 1H), 3.09 (t, J = 7.6 Hz, 2H), 2.80 (t, J = 7.6 Hz, 2H); ^{13}C NMR (101 MHz, DMSO-d_6): 171.43, 154.73, 147.12, 141.49, 138.76, 136.27, 131.04, 130.35, 127.01, 126.42, 125.86, 124.45, 124.26, 122.29, 121.16, 121.01, 120.88, 118.35, 118.25, 118.04, 117.56, 113.52, 112.83, 111.40, 95.49, 37.14, 20.74; HRMS (ESI-MS): Calcd for $C_{27}H_{21}{}^{79}BrN_5O$ [M+H$^+$]: 510.09203, for $C_{27}H_{21}{}^{81}BrN_5O$ [M+H$^+$]: 512.09035. Found: 510.09203, 512.08975.

4.1.16. *N*-(1-(3-Bromophenylamino)-4-cyanoisoquinolin-7-yl)-1*H*-indol-2-carboxamide (18)

Indole-2-acetic acid (0.038 g, 0.235 mmol), oxalyl chloride (20.7 μL, 0.236 mmol), catalytic DMF in 1 mL DCM were stirred for 2 h at 30 °C. 7-Amino-1-(3-bromophenylamino)isoquinoline-4-carbonitrile **7** (20 mg, 0.060 mmol in 0.2 mL of 1-methyl-2-pyrrolidinone) was added and stirred for 2 h at room temperature as described in the procedure for **9**. Column chromatography (EtOAc/petroleum ether, 0.1:0.9 to 0.4:0.6) of the crude product afforded 4 mg of pure (14%) of **18** as a yellow solid. ^{1}H NMR (400 MHz, DMSO-d_6): 11.85 (s, 1H), 10.73 (s, 1H), 10.06 (s, 1H), 9.00 (s, 1H), 8.53 (s, 1H), 8.22 (d, J = 9.0 Hz, 1H), 8.12 (s, 1H), 8.00 (d, J = 8.8 Hz, 1H), 7.82 (d, J = 8.2 Hz, 1H), 7.72 (d, J = 8.0 Hz, 1H), 7.56–7.47 (m, 2H), 7.35 (t, J = 8.0 Hz, 1H),7.29 (d, J = 8.0 Hz, 1H), 7.25 (t, J = 8.0 Hz, 1H), 7.10 (t, J = 7.4 Hz, 1H); ^{13}C NMR (151 MHz, DMSO-d_6): 159.93, 154.69, 147.35, 141.46, 138.30, 137.02, 131.36, 130.94, 130.36, 127.49, 127.02, 125.81, 124.36, 124.04, 121.88, 121.18, 120.61, 120.02, 117.92, 117.46, 114.60, 112.47, 104.41, 95.52, 40.06, 39.94, 39.80, 39.66, 39.52, 39.38, 39.24, 39.10; HRMS (ESI-MS): Calcd for $C_{25}H_{17}{}^{79}BrN_5O$ [M+H$^+$]: 482.06110, for $C_{25}H_{17}{}^{81}BrN_5O$ [M+H$^+$]: 484.05905. Found: 482.06067, 484.05867.

4.2. Biochemical characterization of inhibitor activity

MLCK and calmodulin were purchased from Millipore GmbH, Germany. EGFR was purchased from Invitrogen GmbH, Karlsruhe, Germany. IC_{50} determinations for EGFR kinase were measured with the HTRF® KinEASE™-TK assay kit and for MLCK with HTRF® KinEASE™-STK from Cisbio according to the manufacturer's instructions. For EGFR, biotinylated poly-Glu-Tyr peptide was used as a substrate. In the case of MLCK, the phosphorylation reaction was performed with the peptide substrate STK1. After completion of the kinase reaction, an anti-phosphotyrosine (for EGFR) and anti-phospo-STKS1 (for MLCK) antibody labeled with Europium Cryptate were added to the reaction mixture together with Streptavidin labeled with the fluorophore XL665. The amount of phosphorylation of substrate was then determined by measuring the FRET signal between Europium Cryptate and XL665. ATP concentrations were set at their respective K_m values (9.5 μM for EGFR, 18 μM for MLCK) while 375 nM STK1 substrate was used for MLCK and 50 nM of poly-Glu-Tyr substrate was used for EGFR. Kinase and inhibitor were pre-incubated for 30 min before the reaction was started by addition of ATP and substrate peptide. A Tecan Safire^2 plate reader was used to measure the fluorescence of the samples at 620 nm (Eu-labeled antibody) and 665 nm (XL665 labeled Streptavidin) 60 μs after excitation at 317 nm. The ratio of both intensities was calculated in the presence of eight different inhibitor concentrations (also without inhibitor) and was plotted against inhibitor concentrations and fit to a Hill 4-parameter equation to determine IC_{50} values. At least two independent determinations of each IC_{50} were made, each time in duplicate.

4.3. Modeling

4.3.1. Homology modeling of the kinase domain of human smMLCK

In order to find a suitable structural template for smMLCK, a BLAST search against the PDB-databank was performed. From this search, the structure of the human myosin light chain kinase domain (human myosin light chain kinase family member 4, PDB code: 2X4F) was identified as the closest homolog and was chosen as template for preparation of the homology model. The amino acid sequences of smMLCK and the template were aligned using ClustalW[33] and further processed by Modeller 8v2 (http://salilab.org/modeller). Ten models were built using the model procedure of the program. The resulting models were evaluated for stereochemical quality with PROCHECK.[34] The best solution was taken as the final model for the human smMLCK kinase domain.

4.3.2. Modeling of 11 and 9 into the ATP binding site of MLCK and EGFR

Docking of **11** to the smMLCK homology model was performed manually with COOT[35] using the structure of Erlotinib in complex with EGFR (PDB code: 1M17)[36] as reference. Docking of the irreversible inhibitor **9** to EGFR was done in the same way. In this case, the structure of the cSrc kinase domain with the covalent inhibitor **RL3** (PDB code: 2QLQ)[22] was used as a reference. Images were generated with PyMol v0.98.[37]

4.4. Cellular studies

4.4.1. Cell lines and reagents

81 NSCLC cells were obtained from DSMZ (www.dsmz.de), ATCC (www.atcc.org), and other cell culture collections and were maintained as described previously.[30] Mutational analysis and SNP-arrays were used for routine authentication of the cell lines.[30] Inhibitors were dissolved in DMSO and stored at −80 °C.

4.4.2. Viability assays

Cells were plated into sterile 384-well plates using a Multidrop instrument (www.thermo.com). After 24 h of incubation, compounds were added in 10 threefold serial dilutions using a CyBio Vario pintool (www.cybio.com). Cellular viability was determined after 96 h by measuring the ATP content using the CellTiter-Glo assay (www.promega.com). Half-maximal inhibitory concentrations were then determined using the R package 'GI_{50}'.[38]

4.4.3. Western blotting

Western blotting was carried out as described previously.[39] The following antibodies were used: EGFR, *p*-EGFR (Biosource; USA), anti-rabbit-antibody, anti-mouse (Millipore; Germany).

Acknowledgments

We thank Christian Hedberg and Hans-Dieter Arndt for helpful discussions. Merck Sharp & Dohme, Bayer-Schering Pharma, Merck-Serono and BayerCrop Science are thanked for financial support. The work was supported by the German Federal Ministry for Education and Research through the German National Genome Research Network-Plus (NGFN-Plus) (BMBF Grant 01GS08102).

Supplementary data

Supplementary data (GI_{50} values measured for **9** against 81 NSCLC cell lines) associated with this article can be found, in the online version, at doi:10.1016/j.bmc.2010.11.007.

References and notes

1. Chico, L. K.; Van Eldik, L. J.; Watterson, D. M. *Nat. Rev. Drug Disc.* **2009**, *8*, 892.
2. Rabiller, M.; Getlik, M.; Klüter, S.; Richters, A.; Tückmantel, S.; Simard, J. R.; Rauh, D. *Arch. Pharm. (Weinheim)* **2010**, *343*, 193.
3. Robubi, A.; Waldmann, H.; Rauh, D. *ChemBioChem* **2010**, *11*, 1645.
4. Tohtong, R.; Phattarasakul, K.; Jiraviriyakul, A.; Sutthiphongchai, T. *Prostate Cancer Prostatic Dis.* **2003**, *6*, 212.
5. Zhou, X.; Liu, Y.; You, J.; Zhang, H.; Zhang, X.; Ye, L. *Cancer Lett.* **2008**, *270*, 312.
6. Connell, L. E.; Helfman, D. M. *J. Cell Sci.* **2006**, *119*, 2269.
7. Han, Y. J.; Hu, W. Y.; Chernaya, O.; Antic, N.; Gu, L.; Gupta, M.; Piano, M.; de Lanerolle, P. *Mol. Biol. Cell.* **2006**, *17*, 4039.
8. Blair, S. A.; Kane, S. V.; Clayburgh, D. R.; Turner, J. R. *Lab. Invest.* **2006**, *86*, 191.
9. Sellers, J. R.; Spudich, J. A.; Sheetz, M. P. *J. Cell. Biol.* **1985**, *101*, 1897.
10. Gallagher, P. J.; Herring, B. P.; Griffin, S. A.; Stull, J. T. *J. Biol. Chem.* **1991**, *266*, 23936.
11. Wettschureck, N.; Offermanns, S. *J. Mol. Med.* **2002**, *80*, 629.
12. Even-Ram, S.; Doyle, A. D.; Conti, M. A.; Matsumoto, K.; Adelstein, R. S.; Yamada, K. M. *Nat. Cell. Biol.* **2007**, *9*, 299.
13. Vicente-Manzanares, M.; Zareno, J.; Whitmore, L.; Choi, C. K.; Horwitz, A. F. *J. Cell. Biol.* **2007**, *176*, 573.
14. Fazal, F.; Gu, L.; Ihnatovych, I.; Han, Y.; Hu, W.; Antic, N.; Carreira, F.; Blomquist, J. F.; Hope, T. J.; Ucker, D. S.; de Lanerolle, P. *Mol. Cell. Biol.* **2005**, *25*, 6259.
15. Saitoh, M.; Ishikawa, T.; Matsushima, S.; Naka, M.; Hidaka, H. *J. Biol. Chem.* **1987**, *262*, 7796.
16. Tamura, M.; Nakao, H.; Yoshizaki, H.; Shiratsuchi, M.; Shigyo, H.; Yamada, H.; Ozawa, T.; Totsuka, J.; Hidaka, H. *Biochim. Biophys. Acta* **2005**, *1754*, 245.
17. Lukas, T. J.; Mirzoeva, S.; Slomczynska, U.; Watterson, D. M. *J. Med. Chem.* **1999**, *42*, 910.
18. Nakanishi, S.; Yamada, K.; Kase, H.; Nakamura, S.; Nonomura, Y. *J. Biol. Chem.* **1988**, *263*, 6215.
19. Nakanishi, S.; Kakita, S.; Takahashi, I.; Kawahara, K.; Tsukuda, E.; Sano, T.; Yamada, K.; Yoshida, M.; Kase, H.; Matsuda, Y., et al *J. Biol. Chem.* **1992**, *267*, 2157.
20. Wissner, A.; Mansour, T. S. *Arch. Pharm. (Weinheim)* **2008**, *341*, 465.
21. Blair, J. A.; Rauh, D.; Kung, C.; Yun, C. H.; Fan, Q. W.; Rode, H.; Zhang, C.; Eck, M. J.; Weiss, W. A.; Shokat, K. M. *Nat. Chem. Biol.* **2007**, *3*, 229.
22. Michalczyk, A.; Klüter, S.; Rode, H. B.; Simard, J. R.; Grütter, C.; Rabiller, M.; Rauh, D. *Bioorg. Med. Chem.* **2008**, *16*, 3482.
23. Tsou, H. R.; Mamuya, N.; Johnson, B. D.; Reich, M. F.; Gruber, B. C.; Ye, F.; Nilakantan, R.; Shen, R.; Discafani, C.; DeBlanc, R.; Davis, R.; Koehn, F. E.; Greenberger, L. M.; Wang, Y. F.; Wissner, A. *J. Med. Chem.* **2001**, *44*, 2719.
24. Plowman, G. D.; Culouscou, J. M.; Whitney, G. S.; Green, J. M.; Carlton, G. W.; Foy, L.; Neubauer, M. G.; Shoyab, M. *Proc. Natl. Acad. Sci. U.S.A.* **1993**, *90*, 1746.
25. Klüter, S.; Simard, J. R.; Rode, H.; Pawar, V.; Raaijmakers, H. C. A.; Barf, T. A.; Grütter, C.; Rabiller, M.; Van Otterlo, W. A.; Rauh, D., *ChemBioChem*, in press, doi:10.1002/cbic.201000352.
26. Dacic, S.; Flanagan, M.; Cieply, K.; Ramalingam, S.; Luketich, J.; Belani, C.; Yousem, S. A. *Am. J. Clin. Pathol.* **2006**, *125*, 860.
27. Gazdar, A. F. *Oncogene* **2009**, *28*, S24.
28. Sos, M. L.; Rode, H. B.; Heynck, S.; Peifer, M.; Fischer, F.; Klüter, S.; Pawar, V. G.; Reuter, C.; Heuckmann, J. M.; Weiss, J.; Ruddigkeit, L.; Rabiller, M.; Koker, M.; Simard, J. R.; Getlik, M.; Yuza, Y.; Chen, T. H.; Greulich, H.; Thomas, R. K.; Rauh, D. *Cancer Res* **2010**, *70*, 868.
29. Wissner, A.; Berger, D. M.; Boschelli, D. H.; Floyd, M. B., Jr.; Greenberger, L. M.; Gruber, B. C.; Johnson, B. D.; Mamuya, N.; Nilakantan, R.; Reich, M. F.; Shen, R.; Tsou, H. R.; Upeslacis, E.; Wang, Y. F.; Wu, B.; Ye, F.; Zhang, N. *J. Med. Chem.* **2000**, *43*, 3244.
30. Sos, M. L.; Michel, K.; Zander, T.; Weiss, J.; Frommolt, P.; Peifer, M.; Li, D.; Ullrich, R.; Koker, M.; Fischer, F.; Shimamura, T.; Rauh, D.; Mermel, C.; Fischer, S.; Stückrath, I.; Heynck, S.; Beroukhim, R.; Lin, W.; Winckler, W.; Shah, K.; LaFramboise, T.; Moriarty, W. F.; Hanna, M.; Tolosi, L.; Rahnenführer, J.; Verhaak, R.; Chiang, D.; Getz, G.; Hellmich, M.; Wolf, J.; Girard, L.; Peyton, M.; Weir, B. A.; Chen, T. H.; Greulich, H.; Barretina, J.; Shapiro, G. I.; Garraway, L. A.; Gazdar, A. F.; Minna, J. D.; Meyerson, M.; Wong, K. K.; Thomas, R. K. *J. Clin. Invest.* **2009**, *119*, 1727.
31. Sharma, S. V.; Bell, D. W.; Settleman, J.; Haber, D. A. *Nat. Rev. Cancer* **2007**, *7*, 169.
32. Pawar, V. G.; Sos, M. L.; Rode, H. B.; Rabiller, M.; Heynck, S.; van Otterlo, W. A.; Thomas, R. K.; Rauh, D. *J. Med. Chem.* **2010**, *53*, 2892.
33. Thompson, J. D.; Higgins, D. G.; Gibson, T. J. *Nucleic Acids Res.* **1994**, *22*, 4673.
34. Laskowski, R. A.; Macarthur, M. W.; Moss, D. S.; Thornton, J. M. *J. Appl. Cryst.* **1993**, *26*, 283.
35. Emsley, P.; Cowtan, K. *Acta Crystallogr., Sect. D* **2004**, *60*, 2126.
36. Stamos, J.; Sliwkowski, M. X.; Eigenbrot, C. *J. Biol. Chem.* **2002**, *277*, 46265.
37. DeLano, W. L. http://www.pymol.org, 2002.
38. Frommolt, P.; Thomas, R. K. *BMC Bioinformatics* **2008**, *9*, 475.
39. Sos, M. L.; Koker, M.; Weir, B. A.; Heynck, S.; Rabinovsky, R.; Zander, T.; Seeger, J. M.; Weiss, J.; Fischer, F.; Frommolt, P.; Michel, K.; Peifer, M.; Mermel, C.; Girard, L.; Peyton, M.; Gazdar, A. F.; Minna, J. D.; Garraway, L. A.; Kashkar, H.; Pao, W.; Meyerson, M.; Thomas, R. K. *Cancer Res.* **2009**, *69*, 3256.